
EquiHGNN: Scalable Rotationally Equivariant Hypergraph Neural Networks

Tien Dang

Department of Computer Science
The University of Alabama at Birmingham
Birmingham, Alabama 35294, USA
tien.danganh02@gmail.com

Truong-Son Hy*

Department of Computer Science
The University of Alabama at Birmingham
Birmingham, Alabama 35294, USA
thy@uab.edu

Abstract

Molecular interactions often involve high-order relationships beyond pairwise connections. Hypergraphs enable multi-way interactions, making them well-suited for complex molecular systems. We introduce **EquiHGNN**, an **Equivariant HyperGraph Neural Network** that integrates symmetry-aware representations for molecular modeling. By enforcing the equivariance under transformation groups, EquiHGNN preserves geometric and topological properties, yielding more robust and physically meaningful features. Experiments on small and large molecules show that while high-order interactions add little for small molecules, they consistently outperform 2D graphs on larger ones. Incorporating geometric features further boosts accuracy, underscoring the importance of spatial information in molecular learning. Code: <https://github.com/HySonLab/EquiHGNN/>.

1 Introduction

Molecular systems exhibit complex, high-order interactions such as conjugated π -systems, hydrogen bonding networks, and ring strain effects [1, 2]. Graph Neural Networks (GNNs) have been widely applied to molecular modeling [3] due to their ability to capture relational structures via message passing [4, 5]. However, standard GNNs focus on pairwise interactions and often neglect geometric information such as spatial coordinates, bond angles, and torsional relationships, which are critical for accurate 3D molecular representations. Topological Deep Learning (TDL)[6, 7, 8] extends GNNs by incorporating higher-order structures beyond simple edges. Approaches using simplicial[9], cell [10], combinatorial [6, 11], and hypergraph complexes [12, 13, 14] provide richer relational modeling, achieving strong results across tasks [12, 15, 11, 16]. In parallel, Geometric Deep Learning (GDL)[17] emphasizes equivariance to transformations such as rotations and translations. Recent equivariant architectures[18, 19, 20, 21, 22, 23, 24] integrate geometric priors, ensuring learned features respect 3D spatial symmetries. While symmetry has been explored in simplicial [25] and combinatorial complexes [26], incorporating equivariant features into hypergraphs offers a more scalable and direct framework for modeling complex molecular interactions.

We propose EquiHGNN, a framework that integrates topological and geometric learning while preserving equivariance. Rather than designing new message-passing rules, we initialize hypergraph features with symmetry-aware geometric embeddings and invariant scalars, enabling robust structural modeling. We evaluate EquiHGNN on QM9 [27], OPV [28], PCQM4Mv2 [29], and Molecule3D [30]. Results show strong scalability: higher-order interactions have limited benefit for small molecules but consistently improve large-scale performance, especially when enriched with 3D geometric features.

Our contributions are:

*Corresponding Author

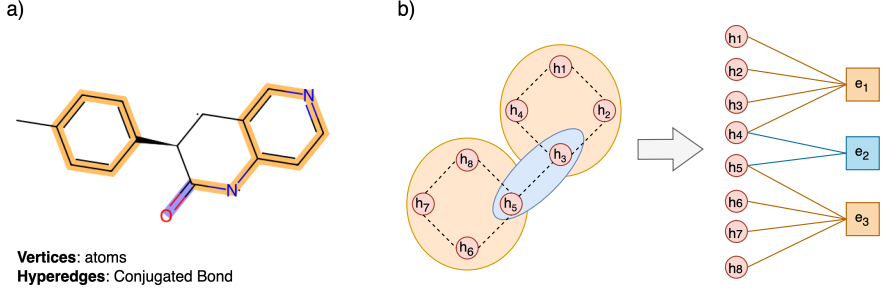


Figure 1: a) Illustration of a hypergraph constructed from a molecule, where vertices represent atoms and hyperedges represent conjugated bonds, highlighted in blue and orange. b) Hypergraph to Bipartite representations

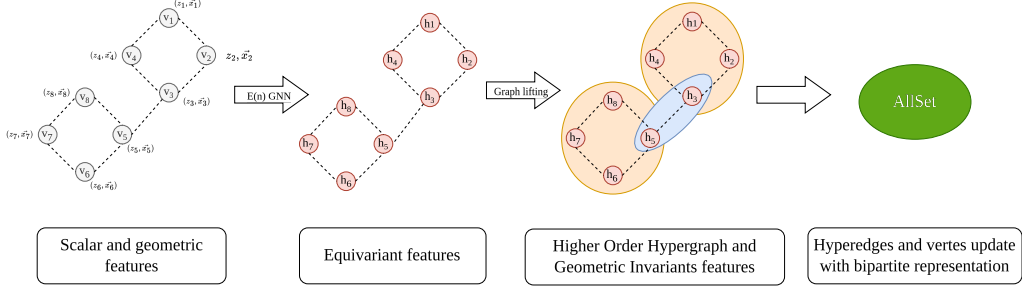


Figure 2: Overview of the Equivariant Hypergraph Neural Network framework.

- Propose EquiHGNN for molecular property prediction, capturing scalar and geometric features in a modular framework.
- Conduct empirical studies with EGNN [31], Equiformer [32], and FAFormer [24] across domains.
- Demonstrate that high-order interactions combined with 3D geometry significantly improve accuracy, particularly on large molecules.

2 Method

This section outlines our approach to modeling high-order interactions with symmetry-aware features and their seamless integration

AllSet. The AllSet framework [13] formulates HGNNs using multiset functions, ensuring permutation invariance and expression of the message passing. It models hypergraphs as bipartite graphs, enabling flexible message propagation through two learnable set functions.

Formally, let $\mathcal{H} = (\mathcal{V}, \mathcal{E})$ be a hypergraph, where \mathcal{V} is the set of nodes and \mathcal{E} is the set of hyperedges, each of which connects a subset of nodes. The AllSet framework updates representations through a two-step message-passing mechanism. First, hyperedge embeddings are computed by aggregating features from incident nodes using a set function $f_{V \rightarrow E}$, defined as follows:

$$Z_e^{(t+1)} = f_{V \rightarrow E} \left(V_{e \setminus v, X^{(t)}}; Z_{e,:}^{(t),v} \right),$$

where $X^{(t)}$ represents the features of nodes in iteration t , $Z_e^{(t)}$ denotes hyperedge embeddings, and V_e is the set of nodes belonging to hyperedge e . This function aggregates node information into a hyperedge representation while preserving permutation invariance.

The node features are then updated based on the embeddings of the hyperedges through a second set function $f_{E \rightarrow V}$, which propagates information back from the hyperedges to the nodes:

$$X_v^{(t+1)} = f_{E \rightarrow V} \left(E_{v, Z_e^{(t+1),v}}; X_{v,:}^{(t)} \right),$$

where E_v is the set of hyperedges containing the node v . This formulation allows the message-passing process to flexibly capture complex dependencies between nodes and hyperedges.

After T steps of the message passing, the hypergraph-level prediction is calculated in the readout part on the final hidden states of hyperedges and nodes:

$$y = \text{MLP} \left(\sum_{v \in G} X_v^{(T)} \sum_{e \in G} Z_e^{(T)} \right).$$

This architecture ensures permutation invariance while allowing expressive transformations of hypergraph features.

Equivariant Hypergraph Neural Network. Our approach extends AllSet by initializing node features with scalar attributes and 3D geometric properties, embedding equivariant information directly into the model. This design yields a more expressive and symmetry-aware framework for hypergraph learning. We evaluate three geometric domains: scalar-based EGNN [31], which preserves distances and invariance; frame-based FAFormer [24], which applies frame averaging to enforce equivariance; and Fourier-based Equiformer [32], which models long-range dependencies in the spectral domain. As shown in Figure 2, symmetry-aware embeddings from these models are used as input features for a hypergraph module that captures higher-order interactions. Hyperedge and vertex features are concatenated and processed by MLP layers to produce predictions. Despite its simplicity, this pipeline substantially improves performance over baselines.

3 Experiments

Density Functional Theory (DFT) is a widely used quantum mechanical method for predicting molecular properties such as structure, reactivity, and electromagnetic responses. While accurate, its cost scales poorly with system size, making large-scale screening impractical and even small molecules time-consuming to compute. To provide efficient alternatives, we evaluate our model on QM9 [27] and OPV [28] for small molecules, and on large-scale datasets PCQM4Mv2 [29] and Molecule3D [30], both derived from PubChemQC [33]. QM9 benchmarks fundamental molecular properties, while OPV focuses on conjugated systems relevant for optoelectronics. PCQM4Mv2 targets HOMO–LUMO gap prediction from SMILES, and Molecule3D emphasizes 3D geometry with property prediction as a secondary task.

3.1 Results

We compare our approach with the MHNN baseline [14], which models hypergraphs as bipartite graphs similar to AllSet [13]. To incorporate symmetry-aware features, we evaluated three setups: EGNN [31], FAFormer [24], and Equiformer [32]. We also benchmark against 2D graph models such as GIN [34] and GAT [35] to assess the benefits of higher-order interactions with symmetry. Across datasets, our models consistently outperform 2D baselines, underscoring the importance of geometric and topological information. The results are summarized in tables with bold for the best and underlined for the second best. For large-scale datasets (PCQM4Mv2, Molecule3D), only EGNN-MHNN is tested due to the cost of training FAFormer and Equiformer. In PCQM4Mv2, experiments are restricted to the training subset where 3D structures are available, ensuring a fair comparison with 2D models. The experimental results of QM9 are included in the Appendix F.

3.1.1 OPV dataset

Table 1: MAE on the OPV test set.

Methods Units (\downarrow)	Molecular				Polymer			
	$\Delta\epsilon$ meV	ϵ_{HOMO} meV	ϵ_{LUMO} meV	I_{overlap} W/mol	$\Delta\epsilon$ meV	ϵ_{HOMO} meV	ϵ_{LUMO} meV	O_{LUMO} meV
GIN	50.45 ± 0.9	39.16 ± 0.5	53.29 ± 0.8	206.53 ± 3.6	53.69 ± 1.0	61.65 ± 0.9	78.48 ± 1.5	64.64 ± 0.6
GAT	55.8 ± 0.9	32.2 ± 0.5	46.68 ± 0.7	204.03 ± 4.2	47.91 ± 0.83	58.47 ± 0.92	71.84 ± 1.3	56.61 ± 0.7
MHNN	34.02 ± 0.4	26.21 ± 0.4	24.46 ± 0.3	139.58 ± 2.3	48.95 ± 1.1	49.93 ± 0.8	60.71 ± 1.1	48.41 ± 0.7
EGNN-MHNN	28.27 ± 0.3	20.97 ± 0.2	20.03 ± 0.3	99.7 ± 1.5	45.63 ± 0.9	66.67 ± 1.1	69.32 ± 1.2	67.28 ± 0.9
FAFormer-MHNN	36.4 ± 0.6	20.5 ± 0.2	18.84 ± 0.3	100.52 ± 1.5	46.12 ± 0.9	54.85 ± 1.0	72.05 ± 1.4	52.74 ± 0.8
Equiformer-MHNN	28.12 ± 0.4	20.24 ± 0.2	20.59 ± 0.3	107.346 ± 1.7	45.42 ± 0.9	50.08 ± 0.8	58.17 ± 1.0	43.6 ± 0.6

The OPV dataset includes both small (molecular) and large (polymer) compounds, offering a robust benchmark for evaluating the scalability and generalization of various graph-based representations. Table 1 highlights the performance (in MAE) of several models in four tasks for each category. For small molecules, the proposed Equiformer-MHNN outperforms all baselines in two out of four tasks. It achieves the lowest MAE for $\Delta\varepsilon$ (28.12 meV) and $\varepsilon_{\text{HOMO}}$ (20.24 meV). FaFormer-MHNN performs best in $\varepsilon_{\text{LUMO}}$ with 18.84 meV, while EGNN-MHNN leads in I_{overlap} . When applied to molecular tasks, incorporating symmetry awareness into the hypergraph consistently outperforms 2D graphs and models that rely solely on higher-order interactions. In contrast, for larger polymer molecules, Equiformer-MHNN continues to demonstrate strong performance, outperforming all other models in three of four tasks. It achieves the best MAE for $\Delta\varepsilon$ (45.42 meV), $\varepsilon_{\text{LUMO}}$ (58.17 meV) and O_{LUMO} (43.6 meV), with a close second for $\varepsilon_{\text{HOMO}}$ (50.08 meV). Although EGNN-MHNN and FAFormer-MHNN do not surpass Equiformer-MHNN, they still significantly outperform traditional 2D GNNs across all polymer-related tasks, highlighting the importance of incorporating geometric and equivariant representations when modeling complex macromolecules. The baseline MHNN, which models high-order interactions without geometric inductive bias, achieves a moderate performance boost over GIN and GAT for small molecules (e.g., 24.46 meV in $\varepsilon_{\text{LUMO}}$ vs 53.29 and 46.68 meV for GIN and GAT, respectively). However, its improvements diminish in the polymer regime, where long-range dependencies and complex geometry require more expressive representations.

3.1.2 PCQM4Mv2 & Molecule3D

Table 2 reports MAE results for PCQM4Mv2 and Molecule3D. On PCQM4Mv2, GIN and GAT record errors of 117.65 and 116.93 meV, while MHNN reduces this to 108.11 meV by modeling high-order interactions. EGNN-MHNN improves further to 98.45 meV, showing that geometric inductive biases improve learning in large-scale molecular graphs. In contrast, on Molecule3D, GIN and GAT reach 129.61 and 137.22 meV, with MHNN achieving the best result (117.55 meV). EGNN-MHNN performs slightly worse (122.25 meV), indicating that geometric modeling may not always help when conformational flexibility is high.

Table 2: MAE on the PCQM4Mv2 and Molecule3D test sets in meV.

Model	PCQM4Mv2 gap (\downarrow)	Molecule3D gap (\downarrow)
GIN	117.65 ± 0.23	129.61 ± 0.25
GAT	116.93 ± 0.21	137.22 ± 0.36
MHNN	<u>108.11 ± 0.25</u>	117.55 ± 0.28
EGNN-MHNN	98.45 ± 0.20	<u>122.25 ± 0.24</u>

4 Conclusion and Future Work

In this work, we integrate symmetry-aware features into hypergraph representations for molecular modeling through a simple yet effective embedding strategy that combines geometric and scalar information. We explored several equivariant techniques, including spatial domain modeling, frame averaging, and Fourier methods, and found that embedding-based initialization is more practical and effective than directly modifying hypergraph message passing. Our results show that hypergraphs consistently outperform pairwise graph approaches on larger molecules, while incorporating symmetry-aware features further improves performance, underscoring the importance of capturing both high-order interactions and geometric consistency.

Despite these strengths, several limitations remain. Beyond conjugated bonds, other high-order interactions, such as those modeled by ETNNs [26] or SE3Set [36] may better capture complex molecular structures, but our experiments with rings showed poor results, suggesting the need for further exploration. Moreover, while advanced equivariant models can surpass Equiformer in efficiency and accuracy, our framework highlights a flexible plug-and-play design where hypergraph node features can be initialized with embeddings from any equivariant backbone. Future work will investigate more effective high-order interactions and integration with state-of-the-art equivariant architectures to further enhance scalability and generalization.

References

- [1] Laurianne David, Amol Thakkar, Rocío Mercado, and Ola Engkvist. Molecular representations in ai-driven drug discovery: a review and practical guide. *Journal of Cheminformatics*, 12(1):56, 2020.
- [2] Daniel S Wigh, Jonathan M Goodman, and Alexei A Lapkin. A review of molecular representation in the age of machine learning. *Wiley Interdisciplinary Reviews: Computational Molecular Science*, 12(5):e1603, 2022.
- [3] Justin Gilmer, Samuel S Schoenholz, Patrick F Riley, Oriol Vinyals, and George E Dahl. Neural message passing for quantum chemistry. In *International conference on machine learning*, pages 1263–1272. PMLR, 2017.
- [4] Marinka Zitnik, Monica Agrawal, and Jure Leskovec. Modeling polypharmacy side effects with graph convolutional networks. *Bioinformatics*, 34(13):i457–i466, 2018.
- [5] Vladimir Gligorijević, P Douglas Renfrew, Tomasz Kosciolek, Julia Koehler Leman, Daniel Berenberg, Tommi Vatanen, Chris Chandler, Bryn C Taylor, Ian M Fisk, Hera Vlamakis, et al. Structure-based protein function prediction using graph convolutional networks. *Nature communications*, 12(1):3168, 2021.
- [6] Mustafa Hajij, Ghada Zamzmi, Theodore Papamarkou, Nina Miolane, Aldo Guzmán-Sáenz, Karthikeyan Natesan Ramamurthy, Tolga Birdal, Tamal K Dey, Soham Mukherjee, Shreyas N Samaga, et al. Topological deep learning: Going beyond graph data. *arXiv preprint arXiv:2206.00606*, 2022.
- [7] Theodore Papamarkou, Tolga Birdal, Michael M. Bronstein, Gunnar E. Carlsson, Justin Curry, Yue Gao, Mustafa Hajij, Roland Kwitt, Pietro Lio, Paolo Di Lorenzo, Vasileios Maroulas, Nina Miolane, Farzana Nasrin, Karthikeyan Natesan Ramamurthy, Bastian Rieck, Simone Scardapane, Michael T Schaub, Petar Veličković, Bei Wang, Yusu Wang, Guowei Wei, and Ghada Zamzmi. Position: Topological deep learning is the new frontier for relational learning. In Ruslan Salakhutdinov, Zico Kolter, Katherine Heller, Adrian Weller, Nuria Oliver, Jonathan Scarlett, and Felix Berkenkamp, editors, *Proceedings of the 41st International Conference on Machine Learning*, volume 235 of *Proceedings of Machine Learning Research*, pages 39529–39555. PMLR, 21–27 Jul 2024.
- [8] Mathilde Papillon, Sophia Sanborn, Mustafa Hajij, and Nina Miolane. Architectures of topological deep learning: A survey of message-passing topological neural networks. *arXiv preprint arXiv:2304.10031*, 2023.
- [9] Cristian Bodnar, Fabrizio Frasca, Yuguang Wang, Nina Otter, Guido F Montufar, Pietro Lio, and Michael Bronstein. Weisfeiler and lehman go topological: Message passing simplicial networks. In *International Conference on Machine Learning*, pages 1026–1037. PMLR, 2021.
- [10] Cristian Bodnar, Fabrizio Frasca, Nina Otter, Yuguang Wang, Pietro Lio, Guido F Montufar, and Michael Bronstein. Weisfeiler and lehman go cellular: Cw networks. *Advances in neural information processing systems*, 34:2625–2640, 2021.
- [11] Mustafa Hajij, Ghada Zamzmi, Theodore Papamarkou, Nina Miolane, Aldo Guzmán-Sáenz, and Karthikeyan Natesan Ramamurthy. Higher-order attention networks. *arXiv preprint arXiv:2206.00606*, 2(3):4, 2022.
- [12] Yihe Dong, Will Sawin, and Yoshua Bengio. Hnnh: Hypergraph networks with hyperedge neurons. *ICML Graph Representation Learning and Beyond Workshop*, 2020.
- [13] Eli Chien, Chao Pan, Jianhao Peng, and Olgica Milenkovic. You are allset: A multiset function framework for hypergraph neural networks. *arXiv preprint arXiv:2106.13264*, 2021.
- [14] Junwu Chen and Philippe Schwaller. Molecular hypergraph neural networks. *The Journal of Chemical Physics*, 160(14):144307, 2024.
- [15] Sergio Barbarossa and Stefania Sardellitti. Topological signal processing over simplicial complexes. *IEEE Transactions on Signal Processing*, 68:2992–3007, 2020.

- [16] Yuzhou Chen, Yulia R Gel, and H Vincent Poor. Bscnets: Block simplicial complex neural networks. In *Proceedings of the aaai conference on artificial intelligence*, volume 36, pages 6333–6341, 2022.
- [17] Michael M Bronstein, Joan Bruna, Taco Cohen, and Petar Veličković. Geometric deep learning: Grids, groups, graphs, geodesics, and gauges. *arXiv preprint arXiv:2104.13478*, 2021.
- [18] Kristof Schütt, Pieter-Jan Kindermans, Huziel Enoc Sauceda Felix, Stefan Chmiela, Alexandre Tkatchenko, and Klaus-Robert Müller. Schnet: A continuous-filter convolutional neural network for modeling quantum interactions. *Advances in neural information processing systems*, 30, 2017.
- [19] Brandon Anderson, Truong Son Hy, and Risi Kondor. Cormorant: Covariant molecular neural networks. In H. Wallach, H. Larochelle, A. Beygelzimer, F. d’Alché-Buc, E. Fox, and R. Garnett, editors, *Advances in Neural Information Processing Systems*, volume 32. Curran Associates, Inc., 2019.
- [20] Simon Batzner, Albert Musaelian, Lixin Sun, Mario Geiger, Jonathan P Mailoa, Mordechai Kornbluth, Nicola Molinari, Tess E Smidt, and Boris Kozinsky. E (3)-equivariant graph neural networks for data-efficient and accurate interatomic potentials. *Nature communications*, 13(1):2453, 2022.
- [21] Shuo Zhang, Yang Liu, and Lei Xie. A universal framework for accurate and efficient geometric deep learning of molecular systems. *Scientific Reports*, 13(1):19171, 2023.
- [22] Yusong Wang, Tong Wang, Shaoning Li, Xinheng He, Mingyu Li, Zun Wang, Nanning Zheng, Bin Shao, and Tie-Yan Liu. Enhancing geometric representations for molecules with equivariant vector-scalar interactive message passing. *Nature Communications*, 15(1):313, 2024.
- [23] Yi-Lun Liao, Brandon Wood, Abhishek Das*, and Tess Smidt*. EquiformerV2: Improved Equivariant Transformer for Scaling to Higher-Degree Representations. In *International Conference on Learning Representations (ICLR)*, 2024.
- [24] Tinglin Huang, Zhenqiao Song, Rex Ying, and Wengong Jin. Protein-nucleic acid complex modeling with frame averaging transformer. In *Neural Information Processing Systems*, 2024.
- [25] Floor Eijkelboom, Rob Hesselink, and Erik J Bekkers. E (n) equivariant message passing simplicial networks. In *International Conference on Machine Learning*, pages 9071–9081. PMLR, 2023.
- [26] Claudio Battiloro, Mauricio Tec, George Dasoulas, Michelle Audirac, Francesca Dominici, et al. E (n) equivariant topological neural networks. *arXiv preprint arXiv:2405.15429*, 2024.
- [27] Raghunathan Ramakrishnan, Pavlo O Dral, Matthias Rupp, and O Anatole Von Lilienfeld. Quantum chemistry structures and properties of 134 kilo molecules. *Scientific data*, 1(1):1–7, 2014.
- [28] Peter C St John, Caleb Phillips, Travis W Kemper, A Nolan Wilson, Yanfei Guan, Michael F Crowley, Mark R Nimlos, and Ross E Larsen. Message-passing neural networks for high-throughput polymer screening. *The Journal of chemical physics*, 150(23), 2019.
- [29] Weihua Hu, Matthias Fey, Hongyu Ren, Maho Nakata, Yuxiao Dong, and Jure Leskovec. Ogb-lsc: A large-scale challenge for machine learning on graphs. *arXiv preprint arXiv:2103.09430*, 2021.
- [30] Zhao Xu, Youzhi Luo, Xuan Zhang, Xinyi Xu, Yaochen Xie, Meng Liu, Kaleb Dickerson, Cheng Deng, Maho Nakata, and Shuiwang Ji. Molecule3d: A benchmark for predicting 3d geometries from molecular graphs. *arXiv preprint arXiv:2110.01717*, 2021.
- [31] Victor Garcia Satorras, Emiel Hoogeboom, and Max Welling. E (n) equivariant graph neural networks. In *International conference on machine learning*, pages 9323–9332. PMLR, 2021.
- [32] Yi-Lun Liao and Tess Smidt. Equiformer: Equivariant graph attention transformer for 3d atomistic graphs. In *International Conference on Learning Representations*, 2023.

- [33] Maho Nakata and Tomomi Shimazaki. Pubchemqc project: a large-scale first-principles electronic structure database for data-driven chemistry. *Journal of chemical information and modeling*, 57(6):1300–1308, 2017.
- [34] Keyulu Xu, Weihua Hu, Jure Leskovec, and Stefanie Jegelka. How powerful are graph neural networks? *arXiv preprint arXiv:1810.00826*, 2018.
- [35] Petar Veličković, Guillem Cucurull, Arantxa Casanova, Adriana Romero, Pietro Liò, and Yoshua Bengio. Graph attention networks. In *International Conference on Learning Representations*, 2018.
- [36] Hongfei Wu, Lijun Wu, Guoqing Liu, Zhirong Liu, Bin Shao, and Zun Wang. Se3set: Harnessing equivariant hypergraph neural networks for molecular representation learning. *arXiv preprint arXiv:2405.16511*, 2024.
- [37] Jie Zhou, Ganqu Cui, Shengding Hu, Zhengyan Zhang, Cheng Yang, Zhiyuan Liu, Lifeng Wang, Changcheng Li, and Maosong Sun. Graph neural networks: A review of methods and applications. *AI open*, 1:57–81, 2020.
- [38] Will Hamilton, Zhitao Ying, and Jure Leskovec. Inductive representation learning on large graphs. *Advances in neural information processing systems*, 30, 2017.
- [39] Thomas N Kipf and Max Welling. Semi-supervised classification with graph convolutional networks. *arXiv preprint arXiv:1609.02907*, 2016.
- [40] Johannes Gasteiger, Janek Groß, and Stephan Günnemann. Directional message passing for molecular graphs. In *International Conference on Learning Representations (ICLR)*, 2020.
- [41] Johannes Gasteiger, Florian Becker, and Stephan Günnemann. Gemnet: Universal directional graph neural networks for molecules. *Advances in Neural Information Processing Systems*, 34:6790–6802, 2021.
- [42] Truong Son Hy. Graph representation learning, deep generative models on graphs, group equivariant molecular neural networks and multiresolution machine learning. page 366.
- [43] Omri Puny, Matan Atzmon, Heli Ben-Hamu, Ishan Misra, Aditya Grover, Edward J Smith, and Yaron Lipman. Frame averaging for invariant and equivariant network design. *arXiv preprint arXiv:2110.03336*, 2021.
- [44] Alexandre Agm Duval, Victor Schmidt, Alex Hernández-García, Santiago Miret, Fragkiskos D Malliaros, Yoshua Bengio, and David Rolnick. Faenet: Frame averaging equivariant gnn for materials modeling. In *International Conference on Machine Learning*, pages 9013–9033. PMLR, 2023.
- [45] Taco S. Cohen, Mario Geiger, Jonas Köhler, and Max Welling. Spherical CNNs. In *International Conference on Learning Representations*, 2018.
- [46] Nathaniel Thomas, Tess Smidt, Steven Kearnes, Lusann Yang, Li Li, Kai Kohlhoff, and Patrick Riley. Tensor field networks: Rotation-and translation-equivariant neural networks for 3d point clouds. *arXiv preprint arXiv:1802.08219*, 2018.
- [47] Fabian Fuchs, Daniel Worrall, Volker Fischer, and Max Welling. Se (3)-transformers: 3d roto-translation equivariant attention networks. *Advances in neural information processing systems*, 33:1970–1981, 2020.
- [48] Johannes Brandstetter, Rob Hesselink, Elise van der Pol, Erik J Bekkers, and Max Welling. Geometric and physical quantities improve e(3) equivariant message passing. In *International Conference on Learning Representations*, 2022.
- [49] Chaitanya K Joshi, Cristian Bodnar, Simon V Mathis, Taco Cohen, and Pietro Lio. On the expressive power of geometric graph neural networks. In *International conference on machine learning*, pages 15330–15355. PMLR, 2023.

- [50] Truong Son Hy, Shubhendu Trivedi, Horace Pan, Brandon M. Anderson, and Risi Kondor. Predicting molecular properties with covariant compositional networks. *The Journal of Chemical Physics*, 148(24):241745, 06 2018.
- [51] Yifan Feng, Haoxuan You, Zizhao Zhang, Rongrong Ji, and Yue Gao. Hypergraph neural networks. In *Proceedings of the AAAI conference on artificial intelligence*, volume 33, pages 3558–3565, 2019.
- [52] Cong Liu, David Ruhe, Floor Eijkelboom, and Patrick Forré. Clifford group equivariant simplicial message passing networks. *arXiv preprint arXiv:2402.10011*, 2024.
- [53] Kevin A Murgas, Emil Saucan, and Romeil Sandhu. Hypergraph geometry reflects higher-order dynamics in protein interaction networks. *Scientific Reports*, 12(1):20879, 2022.
- [54] Philippe Schwaller, Riccardo Petraglia, Valerio Zullo, Vishnu H Nair, Rico Andreas Haeuselmann, Riccardo Pisoni, Costas Bekas, Anna Iuliano, and Teodoro Laino. Predicting retrosynthetic pathways using transformer-based models and a hyper-graph exploration strategy. *Chemical science*, 11(12):3316–3325, 2020.
- [55] Justin Airas and Bin Zhang. Scaling graph neural networks to large proteins. *Journal of Chemical Theory and Computation*, 2024.
- [56] Matthias Fey and Jan E. Lenssen. Fast graph representation learning with PyTorch Geometric. In *ICLR Workshop on Representation Learning on Graphs and Manifolds*, 2019.

A Related Work

A.1 Graph Neural Network

Graph Neural Networks (GNNs) have been widely developed to improve representation learning in graph-structured data, enabling effective modeling of relational and structural information [37]. GraphSAGE [38] introduced an inductive framework that aggregates information from the local neighborhood of a node, allowing generalization to unseen graphs. More general, Message Passing Neural Networks (MPNNs) [3] are a foundational class of GNNs that iteratively update node representations by aggregating and transforming information from their neighbors, enabling effective learning on graph-structured data. Graph Convolutional Networks (GCN) [39] leveraged spectral graph theory to perform efficient message passing through neighborhood-based feature propagation. Graph Isomorphism Networks (GIN) [34] maximized expressive power by using sum aggregation, making them as discriminative as the Weisfeiler-Lehman test for graph isomorphism. Graph Attention Networks (GAT) [35] integrated attention mechanisms to dynamically weight neighbor contributions, improving the model’s ability to capture important structural dependencies. However, these models operate on discrete graph structures, lack inherent equivariance or invariance to geometric transformations such as rotations, translations, and reflections, and can only model pairwise interactions, making them impractical for capturing high-order molecular interactions such as conjugate bonds. This work addresses these limitations by proposing EquiHGNN, a framework that incorporates both geometric awareness and higher-order interaction modeling.

A.2 Geometric Graph Neural Networks

Geometric graph [17] is a special kind of graph with geometric information, e.g. the positions of the atoms in 3D coordinates, encapsulating rich directional information that depicts the geometry of the system, making the system ineffectively processed by GNNs. Researchers propped a variety of Geometric Graph Neural Networks quipped with invariant/equivariant properties to better characterize the geometry of geometric graph.

Many tasks require models to be invariant under Euclidean transformations, which is often achieved by converting equivariant coordinates into invariant scalars. Early works like Cormorant [19] introduced the idea of using covariant tensorial representations for molecular graphs, ensuring that the learned features transform predictably under rotations and translations. Using spherical harmonics and tensor contractions, Cormorant demonstrated how symmetry-preserving architectures can substantially improve molecular property predictions. SchNet [18] uses continuous filter convolutions with filter weights conditioned on relative distances but lacks directional encoding. DimeNet [40] addresses this by introducing directional message passing, incorporating both distances and angles between adjacent edges. GemNet [41] extends this further by incorporating dihedral angles, enabling more expressive two-hop directional message passing based on quadruplets of nodes.

Equivariant graph neural networks, on the contrary, simultaneously update invariant and equivariant features, as many tasks require equivariant output [42]. EGNN [31], a well-known scalarization-based model, constrains messages to invariant distances and multiplies them by relative coordinates to ensure equivariant updates. Frame Averaging (FA) [43, 44] ensures equivariance by encoding coordinates in multiple reference frames and averaging their representations. Since summing over all group elements is computationally difficult, FA selects a representative subset using a frame function [43]. This method has been further explored in material design, offering a scalable alternative to traditional equivariant architectures [44]. FAFormer [24] incorporates the Transformer with frame averaging within each layer, offers superior performance in the prediction of contact maps and the detection of aptamers.

Spherical harmonics-based models use functions derived from spherical harmonics and irreducible representations, leveraging tensor product operations to ensure equivariant data transformations [45, 19]. Tensor Field Network (TFN) [46] and NequIP[20] utilize equivariant graph convolutions with linear messages derived from tensor products, with NequIP further enhancing this approach using equivariant gate activations. The SE(3)-Transformer [47] extends SEGNN [48] by replacing equivariant gate activations with equivariant dot product attention for dynamic interaction weighting, while Equiformer [32] further enhances it with MLP-based attention, equivariant layer normalization, and regularizations such as dropout and stochastic depth.

As shown in [49], rotationally equivariant GNNs are more expressive than invariant GNNs, especially for sparse geometric graphs. In this work, we focus on equivariant methods, specifically EGNN [31] for the scalarization-based approach, FAFormer [24] for the frame-averaging-based approach, and Equiformer [32] for the spherical harmonic-based approach.

A.3 Topological Deep Learning

Topological Deep Learning (TDL) [6, 7] extends beyond traditional graphs by leveraging higher-order structures, enabling a more expressive framework for modeling complex interactions among multiple entities simultaneously. Beyond rotational symmetry, molecular graphs also exhibit rich permutation symmetries in their relational structure. Predicting molecular properties with Covariant Compositional Networks (CCNs) [50] proposed a framework that preserves higher-order permutation equivariance during message passing by modeling interactions as higher-order tensors. This approach enables the network to learn more expressive and physically meaningful representations compared to first-order (pairwise) GNNs, especially when modeling complex molecular systems with many-body interactions. The Weisfeiler-Lehman graph isomorphism test has been extended to simplicial and regular cell complexes [9, 10], providing a theoretical foundation for higher-order graph structures. HGNN [51] introduced a spectral-based framework that utilizes the Laplacian hypergraph to pass messages across hyperedges. To improve flexibility, AllSet [13] proposed a more general approach that models hypergraphs as multi-sets, employing learnable permutation-invariant set functions for adaptive message aggregation. Compared to baseline pretrained GNNs, MHNN [14] takes advantage of the hypergraph to achieve better performance under limited training data. CCNN [6] further advances this direction by introducing Combinatorial Complexes, which capture hierarchical order and enable structured dependencies across multiple levels. A comprehensive review of these advances can be found in [8].

Despite these developments, there has been limited work that incorporates symmetry with topological structures. Recent efforts have explored simplicial complexes with equivariant message passing [25, 52], integrating symmetry-aware mechanisms into higher-order networks [52]. Additionally, ETNN [26] extends equivariant message passing to combinatorial complexes, providing a more structured approach to learning equivariant representations in topological deep learning.

Hypergraphs offer a powerful framework for modeling higher-order interactions, particularly in domains such as molecular modeling and complex systems. However, equivariant hypergraph neural networks remain largely unexplored. This work introduces a novel hypergraph-equivariant framework that inherits the scalability of graph-based methods, making it suitable for large molecular systems, while also incorporating equivariant geometric features to enhance expressive power and robustness.

B Background

B.1 Message Passing

Message Passing Neural Networks (MPNNs) play a fundamental role in learning node representations by propagating information along graph edges. As inherently permutation-invariant architectures, MPNNs effectively capture relational structures in graph-structured data, making them particularly well-suited for applications such as molecular modeling [3].

Given a graph $\mathcal{G} = (\mathcal{V}, \mathcal{E})$ with nodes $v_i \in \mathcal{V}$ and edges $e_{ij} \in \mathcal{E}$, each node v_i is associated with a feature vector $\mathbf{h}_i \in \mathbb{R}^{c_n}$ and each edge e_{ij} with a feature vector $\mathbf{a}_{ij} \in \mathbb{R}^{c_e}$, where c_n and c_e represent the dimensionalities of the node and edge features, respectively. The nodes representation are iteratively updated by:

$$\begin{aligned} \mathbf{m}_{ij} &= \phi_e(\mathbf{h}_i^l, \mathbf{h}_j^l, \mathbf{a}_{ij}) \\ \mathbf{m}_i &= \text{AGGREGATE}\left(\{\mathbf{m}_{ij}\}_{j \in \mathcal{N}(i)}\right) \\ \mathbf{h}_i^{l+1} &= \phi_u(\mathbf{h}_i^l, \mathbf{m}_i) \end{aligned} \tag{1}$$

where $\mathcal{N}(i)$ denotes the set of neighbors of node v_i , and the AGGREGATE function is a permutation-invariant operation over the neighbors (e.g., summation). The functions ϕ_m and ϕ_e are the message computation and the feature update function, respectively, typically parameterized by multilayer

Table 3: Model Architecture Overview

Model	No. parameters	No.layers	No. attention heads	Hidden dimension
GIN	965K	2	-	256
GAT	3.7M	2	4	256
MHNN	2.5M	2	-	256
EGNN	844K	2	8	256
FAFormer	3.2M	2	2	256
Equiformer	13M	1	1	256

perceptrons (MLP). To obtain the final graph representation, a permutation-invariant aggregator is applied to the final hidden states of all nodes. However, this operation itself does not inherently preserve the $E(3)$ equivariance.

B.2 Equivariance

Equivariance is a property of functions that ensures that information is preserved under transformations from a group G . A function $\phi : \mathcal{X} \rightarrow \mathcal{Y}$ is equivariant with respect to G if for all $g \in G$ and $x \in \mathcal{X}$, the following holds:

$$\phi(g \cdot x) = g \cdot \phi(x).$$

This property ensures that the output transforms in the same way as the input under transformations like rotation, translation, or scaling. In molecular modeling, the equivariance with these symmetries (e.g., the rotation group $SO(3)$) is crucial because molecules retain their physical properties regardless of their orientation or position.

B.3 Hypergraph

A *hypergraph* is a generalization of a graph where an edge, called a *hyperedge*, can connect any number of nodes. Formally, a hypergraph is defined as:

$$\mathcal{H} = (\mathcal{V}, \mathcal{E}),$$

where \mathcal{V} is the set of nodes and $\mathcal{E} \subseteq 2^{\mathcal{V}} \setminus \{\emptyset\}$ is the set of hyperedges, each representing a subset of nodes. Unlike traditional graphs that capture pairwise relationships, hypergraphs model higher-order interactions, making them ideal for complex systems such as protein interactions [53] and chemical reactions [54].

Hypergraph-based models extend GNNs to process hyperedges, allowing better representation of structured data. In molecular chemistry, hypergraphs effectively model *conjugated structures*, where delocalized electrons form multi-atomic interactions crucial for optoelectronic properties. Recent studies demonstrate that HGNNs outperform traditional GNNs and 3D-based models in predicting molecular properties, offering a powerful approach for data-scarce applications like organic semiconductor design.

C Model details

Table 3 outlines the architectural configurations of the models used in our experiments, including the number of parameters, layers, attention heads, and hidden dimensions.

D Datasets

QM9 [27] dataset is a widely used reference for the prediction of chemical properties. It comprises approximately 134,000 small organic molecules, each containing up to 29 atoms. The data set includes five atomic species including hydrogen, carbon, oxygen, nitrogen, and fluorine, structured as molecular graphs where the atoms are connected by four types of chemical bonds: single, double,

Table 4: Overview of the datasets

Dataset	Graphs	Task type	Task number	Metric
QM9	134K	regression	12	MAE
OPV	91K	regression	8	MAE
PCQM4Mv2	3.7M	regression	1	MAE
Molecule3D	3.9M	regression	6	MAE

triple, and aromatic. In addition, the 3D coordinates of each atom, measured in angstroms, are provided.

Organic Photovoltaic (OPV) [28] comprises 90,823 unique molecules, providing their SMILES representations, 3D geometries, and optoelectronic properties computed by DFT calculations. It includes four molecular-level tasks for monomers: the highest occupied molecular orbital ($\varepsilon_{\text{HOMO}}$), the lowest unoccupied molecular orbital ($\varepsilon_{\text{LUMO}}$), the HOMO-LUMO gap ($\Delta\varepsilon$), and the spectral overlap (I_{overlap}). Furthermore, OPV features four polymer-level tasks: polymer $\varepsilon_{\text{HOMO}}$, polymer $\varepsilon_{\text{LUMO}}$, the polymer energy gap ($\Delta\varepsilon$), and the optical LUMO (O_{LUMO}).

PCQM4Mv2 [29] is a large-scale quantum chemistry dataset consisting of approximately 3.7 million molecular graphs, derived from the PubChemQC project [33]. It is designed for predicting the DFT-calculated HOMO-LUMO energy gap from SMILES representations, and additionally provides 3D structures for the training molecules.

Molecule3D [30] is a large-scale benchmark designed to predict 3D molecular geometries from 2D molecular graphs and to assess their effectiveness in downstream prediction of quantum properties. It supports two main tasks: (1) prediction of DFT-optimized 3D atomic coordinates from SMILES strings or molecular graphs, and (2) prediction of quantum properties such as total energy, HOMO/LUMO energies, and the HOMO–LUMO gap using either ground truth or predicted 3D structures. Each sample includes a SMILES string, molecular graph, 3D coordinates, and quantum properties sourced from PubChemQC [33]. In this work, we focus specifically on the prediction of the HOMO-LUMO gap.

Table 4 provides an overview of the experimental dataset. We use RDKit to identify conjugated bonds, which serve as hyperedges, with atoms as vertices, as illustrated in Section 1a. For all experiments, the data are split into training, validation and test sets using an 80-10-10 ratio. The model is trained in the training set, the best model is selected based on the performance in the validation set, and the final evaluation is performed in the test set.

E Training details

Equivariant models utilize radial distances, where a larger radius enables the capture of high-level features crucial for complex molecules such as polymers and proteins. In such molecules, long-range interactions, such as electrostatic and hydrophobic effects, are key to determining their electronic and structural properties. A study on scaling GNNs [55] shows that increasing the number of message-passing layers and the cutoff radius helps GNNs incorporate distant atomic interactions, thereby enhancing expressiveness for large proteins.

However, in transformer-based architectures, a larger radius significantly increases computational costs due to the quadratic scaling of the attention mechanism with the number of nodes. Based on these empirical insights, we adopt a consistent configuration with a 5 Angstrom radius cutoff and 16 neighboring nodes for EGN, FAFormer, and Equiformer, achieving an optimal balance between expressiveness and computational efficiency. Appendix C provides a summary of the model architecture configurations.

We train the models for 400 epochs with a batch size of 16, using the Adam optimizer with a fixed learning rate of 1×10^{-4} . Training is carried out on 2xRTX 3060 GPUs, enabling parallel processing for efficiency. The models are optimized to minimize the loss of MSE, and the checkpoint with the lowest MAE validation is selected for the final evaluation on the test set. Our implementation is built using PyTorch Geometric [56].

F Additional results on QM9

Table 5: MAE on the QM9 test set.

Task Units (\downarrow)	μ D	α a_0^3	ϵ_{HOMO} meV	ϵ_{LUMO} meV	$\Delta\epsilon$ meV	$\langle R^2 \rangle$ a_0^2
GIN	0.2 ± 0.003	4.09 ± 0.04	47.67 ± 0.4	99.62 ± 0.9	147.87 ± 1.3	6279.8 ± 86.91
GAT	0.65 ± 0.006	6.17 ± 0.07	51.56 ± 0.5	111.24 ± 0.9	158.26 ± 1.1	8772.5 ± 97.43
MHNN	0.67 ± 0.005	9.29 ± 0.1	55.38 ± 0.5	124.23 ± 1.07	166.6 ± 1.3	9301.44 ± 138.369
EGNN-MHNN	0.59 ± 0.005	2.02 ± 0.02	44.82 ± 0.3	92.54 ± 0.9	<u>140.06 ± 1.5</u>	<u>4293.09 ± 66.44</u>
FAFormer-MHNN	<u>0.3 ± 0.003</u>	4.85 ± 0.04	<u>26.47 ± 0.2</u>	51.9 ± 0.4	73.3 ± 0.7	2602.89 ± 25.04
Equiformer-MHNN	0.34 ± 0.003	<u>2.48 ± 0.02</u>	25.57 ± 0.2	<u>67.19 ± 0.5</u>	230.77 ± 1.8	102815 ± 445.433

Table 5 presents the Mean Absolute Error (MAE) for six molecular properties from the QM9 dataset. The baseline MHNN, which captures higher-order interactions through hypergraph representations, underperforms compared to standard 2D graph-based models. For example, on ϵ_{HOMO} , MHNN yields an MAE of 55.38 meV, while GIN and GAT achieve 47.67 meV and 51.56 meV, respectively. GIN also records the lowest error on μ (0.2 meV). These results suggest that modeling higher-order relations alone does not improve the performance of small molecules. In contrast, incorporating geometric inductive biases leads to significant gains. Both EGNN-MHNN and FAFormer-MHNN consistently reduce MAE across tasks. FAFormer-MHNN achieves the best results in three of the six properties, including ϵ_{LUMO} (51.9 meV), $\Delta\epsilon$ (73.3 meV), and $\langle R^2 \rangle$ (2602.89 a_0^2), halving the error compared to the baselines of the MHNN and 2D graph. EGNN-MHNN obtains the lowest MAE in α (2.02 a_0^3) and competitive results on $\langle R^2 \rangle$ (4293.09 a_0^2). In particular, Equiformer-MHNN achieves the best performance in ϵ_{HOMO} (25.57 meV). These findings highlight that while higher-order modeling alone is insufficient, combining topological and geometric priors yields a more powerful and accurate framework for molecular property prediction in the QM9 setting.